A&A 607, A69 (2017)
DOI: 10.1051/0004-6361/201730585

Astronomy & Astrophysics

Super-spinning compact objects and models of high-frequency quasi-periodic oscillations observed in Galactic microquasars

II. Forced resonances

A. Kotrlová[1], E. Šrámková[1], G. Török[1], Z. Stuchlík[2], and K. Goluchová[1,2,3]

[1] Institute of Physics and Research Centre for Computational Physics and Data Processing, Faculty of Philosophy & Science, Silesian University in Opava, Bezručovo nám. 13, 746 01 Opava, Czech Republic
e-mail: Andrea.Kotrlova@fpf.slu.cz
[2] Institute of Physics and Research Centre for Theoretical Physics and Astrophysics, Faculty of Philosophy & Science, Silesian University in Opava, Bezručovo nám. 13, 746 01 Opava, Czech Republic
[3] Nicolaus Copernicus Astronomical Centre, Bartycka 18, 00716 Warsaw, Poland

Received 9 February 2017 / Accepted 11 July 2017

ABSTRACT

In our previous work (Paper I) we applied several models of high-frequency quasi-periodic oscillations (HF QPOs) to estimate the spin of the central compact object in three Galactic microquasars assuming the possibility that the central compact body is a super-spinning object (or a naked singularity) with external spacetime described by Kerr geometry with a dimensionless spin parameter $a \equiv cJ/GM^2 > 1$. Here we extend our consideration, and in a consistent way investigate implications of a set of ten resonance models so far discussed only in the context of $a < 1$. The same physical arguments as in Paper I are applied to these models, i.e. only a small deviation of the spin estimate from $a = 1$, $a \gtrsim 1$, is assumed for a favoured model. For five of these models that involve Keplerian and radial epicyclic oscillations we find the existence of a unique specific QPO excitation radius. Consequently, there is a simple behaviour of dimensionless frequency $M \times \nu_{\rm U}(a)$ represented by a single continuous function having solely one maximum close to $a \gtrsim 1$. Only one of these models is compatible with the expectation of $a \gtrsim 1$. The other five models that involve the radial and vertical epicyclic oscillations imply the existence of multiple resonant radii. This signifies a more complicated behaviour of $M \times \nu_{\rm U}(a)$ that cannot be represented by single functions. Each of these five models is compatible with the expectation of $a \gtrsim 1$.

Key words. X-rays: binaries – black hole physics – accretion, accretion disks

1. Introduction

Accreting black holes (BHs) or neutron stars (NSs) are believed to constitute the compact component in several tens of X-ray binaries. The accretion disc contributes significantly to the high X-ray luminosity of these objects. Most of the X-ray radiation comes from the inner parts of the disc. Both the BH and NS sources exhibit a variability over a wide range of frequencies. In addition to broad noise, their power density spectra (PDS) also contain relatively coherent features known as quasi-periodic oscillations (QPOs). A brief introduction to the subject of QPOs can be found in van der Klis (2006) and McClintock & Remillard (2006).

The X-ray PDS of several stellar mass BH systems display low-frequency (LF) QPOs in the range of 0.1–30 Hz. Their strength expressed in terms of the fractional root-mean-squared (rms) amplitude $\mathcal{R}$ is sometimes as high as $\mathcal{R} \sim 20\%$. Much attention among theoreticians is, however, attracted to high-frequency (HF or kHz) QPOs that display their frequencies within the range of 40–450 Hz. High-frequency QPOs usually display much smaller amplitudes than LF QPOs, $\mathcal{R} \sim 1$–4%, but their frequencies correspond to orbital timescales in the vicinity of a BH. It is believed that this coincidence is a strong indication that the corresponding signal originates in the innermost parts of the accretion disc. This belief has also been supported by means of the Fourier-resolved spectroscopy (e.g. Gilfanov et al. 2000).

The kHz QPO peaks are detected at rather constant frequencies characteristic for a given source. Moreover, it has been noticed (Abramowicz & Kluźniak 2001; McClintock & Remillard 2006) that they usually appear in ratios of small natural numbers, typically in the 3:2 ratio. Discussion of these measurements and their relation to other sources can be found in McClintock & Remillard (2006), Török et al. (2005), Török (2005a), and van der Klis (2006). It has been noticed that the 3:2 frequencies observed in the Galactic microquasars are well matched by the relation (e.g. McClintock & Remillard 2006)

$$\nu_{\rm L} = 1.862 \left(\frac{M}{M_\odot}\right)^{-1} \text{kHz}, \tag{1}$$

where $\nu_{\rm L}$ is the lower of the two frequencies forming the 3:2 ratio,

$$R = \nu_{\rm U}/\nu_{\rm L} = 3/2. \tag{2}$$

This scaling of QPO frequencies further supports the hypothesis of their orbital origin (e.g. Török et al. 2005).

There is a common conviction in the astrophysical community that studying X-ray spectra and variability can be used to put constraints on the properties of compact objects such as BH mass M and spin $a \equiv cJ/GM^2$. A standard way to measure the BH spin is based on different spectral fitting methods, namely by fitting the X-ray spectral continuum or the relativistically broadened Fe K alpha lines. Using these spectral

fitting methods, many authors have carried out estimations of BH spin (see e.g. McClintock & Remillard 2006; Middleton et al. 2006; Done et al. 2007; McClintock et al. 2007; Miller 2007; Shafee et al. 2008; McClintock et al. 2010, 2011, 2014).

Abramowicz et al. (2004) have suggested that detections of 3:2 QPOs could provide a basis for another method for the determination of masses of BH sources such as the active galactic nuclei and ultraluminous X-ray sources. This suggestion is further supported by Török (2005a,b) who has discussed the possibility of orbital resonance origin of QPOs in the Galactic centre BH Sagittarius A* measured by Aschenbach et al. (2004). It has been argued that the confirmation of 3:2 QPOs in this source could be of fundamental importance to the BH accretion theory. At present, a full decade after these results were published and even though Sgr A* QPO detections remain questionable, there is a growing evidence of the existence of a large-scale validity of the $1/M$ scaling of the BH QPO frequencies (1) (see e.g. Zhou et al. 2015).

For a BH candidate which displays HF QPOs and whose mass has been measured by independent measurements, the BH spin estimate can in principle be obtained by simply comparing the observed QPO frequencies to QPO frequencies predicted by a particular QPO model. Through this approach, using miscellaneous QPO models, a number of authors have attempted to estimate the spin of the central Kerr BH in three Galactic microquasars – GRS 1915+105, XTE J1550−564, and GRO J1655−40 – that display the 3:2 twin peak QPOs and have known masses (e.g. Abramowicz & Kluźniak 2001; Wagoner et al. 2001; Kato 2004; Török 2005b; Wagoner 2012; Horák & Lai 2013; Ortega-Rodríguez et al. 2014; Motta et al. 2014; Stuchlík & Kološ 2016a,b).

This approach can also be applied in the context of testing hypotheses alternative to consideration of Kerr BHs (Török & Stuchlík 2005; Kotrlová et al. 2008; Psaltis et al. 2008; Bambi & Freese 2009; Gimon & Hořava 2009; Stuchlík & Kotrlová 2009; Stuchlík & Schee 2010, 2012a,b, 2013; Bambi 2011; Johannsen & Psaltis 2011; Li & Bambi 2013a,b; Bambi 2012, 2014; Kološ & Stuchlík 2013; Yagi & Stein 2016; Johannsen 2016). Here we focus on the QPO based spin estimates of compact object properties, in particular on those assuming orbital resonances in Kerr spacetimes.

2. Estimates of spin in Galactic microquasars and forced resonances

Orbital resonances have been proposed as a generic QPO mechanism in the works of Abramowicz & Kluźniak (2001) and Kluźniak & Abramowicz (2001), and previously discussed in the general framework of orbital motion by Aliev & Galtsov (1981). Several consequent studies have elaborated this proposal (e.g. Abramowicz et al. 2002; Kluźniak & Abramowicz 2002, 2005; Abramowicz et al. 2003a,b; Rebusco 2004; Horák 2004, 2005; Šrámková 2005; Horák & Karas 2006; Vio et al. 2006; Šrámková et al. 2007; Horák 2008; Rebusco 2008; Stuchlík et al. 2008; Horák et al. 2009; Stuchlík et al. 2013, 2014)[1]. In the works of Kluźniak & Abramowicz (2001) and Török et al. (2005), spin estimates have been carried out for the three microquasars based on a group of QPO models that deal with a non-linear resonance between some modes of accretion disc oscillations. In particular, Török et al. (2005) have discussed resonances that occur between axisymmetric radial and vertical disc oscillations and that may also involve Keplerian motion.

Assuming fluid-disc-oscillation frequencies, it is expected that resonances occur at preferred resonant orbits (QPO excitation radii), $r_{p:q}$ or $\tilde{r}_{p:q}$, where the vertical and radial epicyclic frequency, $\nu_{\rm r}$ and ν_θ, or the Keplerian ($\nu_{\rm K}$) and radial epicyclic frequency are in ratios of small rational numbers,

$$\nu_\theta(r_{p:q}) = \left(\frac{p}{q}\right)\nu_{\rm r}(r_{p:q}), \tag{3}$$

$$\nu_{\rm K}(\tilde{r}_{p:q}) = \left(\frac{p}{q}\right)\nu_{\rm r}(\tilde{r}_{p:q}). \tag{4}$$

The 3:2 ratio of the observed frequencies then arises either from the generic 3:2 ratio of the resonant eigenfrequencies or due to resonant combinational frequencies. The well-known explicit formulae for epicyclic frequencies in Kerr spacetimes have been discussed in several works (e.g. Aliev & Galtsov 1981; Nowak & Lehr 1999; Török & Stuchlík 2005). The behaviour of orbital frequencies and the positions of several specific resonant orbits are illustrated in Fig. 1 assuming two different values of a corresponding to BH and non-BH Kerr spacetimes. For a fixed a, these frequencies scale with the compact object mass M as $\nu \propto 1/M$.

Consideration of Kerr BHs and superspinars (or naked singularities) and resonance QPO models. Several variations of resonance models have been assumed by Török et al. (2005). These consist of both parametric and forced non-linear resonances, in particular the 3:2 parametric resonance, and the 3:1, 2:1, 5:1, 5:2, 5:3 forced resonances. The two most popular alternatives are under consideration: the epicyclic resonance (Ep) model dealing with radial and vertical epicyclic oscillations and the Keplerian resonance (Kep) model assuming a resonance between the orbital Keplerian motion and the radial epicyclic oscillations.

Further complex analysis of spin estimations has been done by Török et al. (2011) for a set of various QPO models. It has been performed namely for hot-spot-like models, models assuming a certain form of resonance between some accretion disc oscillatory modes, and for discoseismic models. Individual models considered in Török et al. (2005, 2011) point to very different values of a covering the whole BH range $a \in [0, 1]$. The iron-line profile, X-ray continuum, and the QPO based spin estimates reveal good agreement only in certain particular applications (e.g. Steiner et al. 2011). There are still discrepancies, and no agreement between the three approaches has been achieved so far (see e.g. Török et al. 2011; Kotrlová et al. 2014).

In Kotrlová et al. (2014, hereafter Paper I) we extended the consideration of QPO based spin estimates to the non-BH case and investigated the behaviour of $M \times \nu_{\rm U}(a)$ relations implied by individual QPO models for $a > 1$. We discussed various types of models including several resonance models and concluded that the Ep and Kep models are favoured in the context of the $a > 1$ hypothesis. In Paper I, our consideration did not include forced resonances investigated by Török et al. (2005) for Kerr BHs. Here we explore the predictions of ten of the forced resonance models mentioned above. The list of these models together with associated relations giving observable QPO frequencies is given in Table 1.

[1] These works often assume the formation of an inner accretion torus, which is frequently considered in the context of the generic QPO mechanism; see also Rezzolla et al. (2003), Zanotti et al. (2005), Schnittman & Rezzolla (2006), Montero et al. (2007), Ingram et al. (2009), Ingram & Done (2010, 2011), Ingram et al. (2016), Török et al. (2016) and references therein.

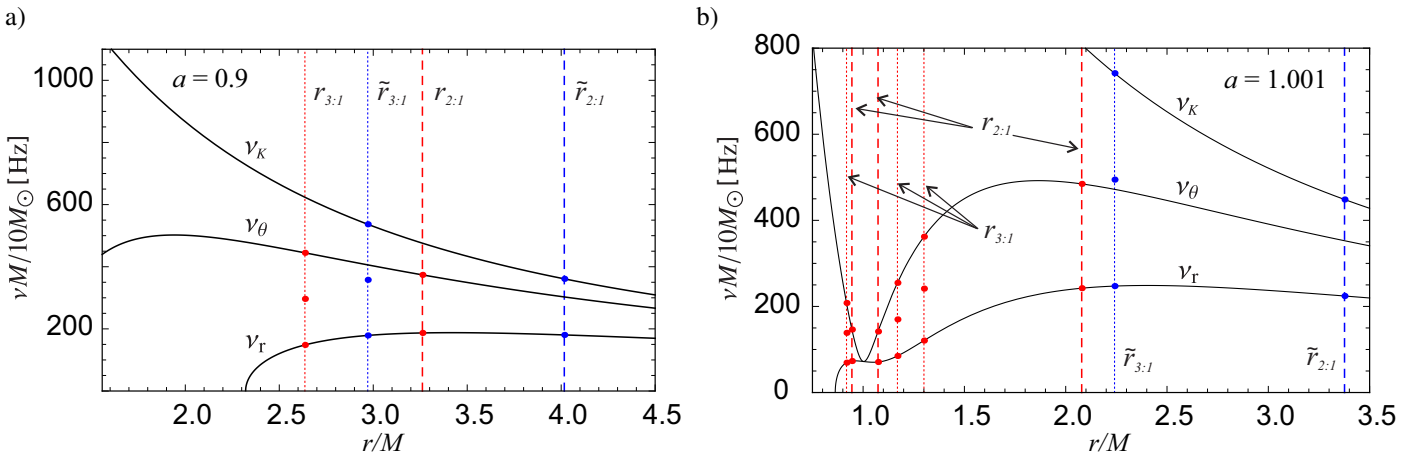

Fig. 1. *Panel a*: behaviour of orbital frequencies and location of several resonant radii determined by the Ep and Kep models for $a = 0.9$. *Panel b*: behaviour of orbital frequencies and location of several resonant radii determined by the Ep and Kep models for $a = 1.001$. For Kerr black holes there is only one specific resonant radius for each displayed resonance, while even three resonant radii may appear for a single Ep model in the case of a super-spinning compact object or naked singularity.

Table 1. Frequency relations corresponding to individual epicyclic and Keplerian forced resonance models.

Model	Type of resonance	Relations		ν_θ/ν_r or ν_k/ν_r
Ep1	epicyclic 3:1 forced	$\nu_L = \nu_\theta - \nu_r$	$\nu_U = \nu_\theta$	3/1
Kep1	Keplerian 3:1 forced	$\nu_L = \nu_k - \nu_r$	$\nu_U = \nu_k$	3/1
Ep2	epicyclic 2:1 forced	$\nu_L = \nu_\theta$	$\nu_U = \nu_\theta + \nu_r$	2/1
Kep2	Keplerian 2:1 forced	$\nu_L = \nu_k$	$\nu_U = \nu_k + \nu_r$	2/1
Ep3	epicyclic 5:1 forced	$\nu_L = \nu_\theta - \nu_r$	$\nu_U = \nu_\theta + \nu_r$	5/1
Kep3	Keplerian 5:1 forced	$\nu_L = \nu_k - \nu_r$	$\nu_U = \nu_k + \nu_r$	5/1
Ep4	epicyclic 5:2 forced	$\nu_L = \nu_r$	$\nu_U = \nu_\theta - \nu_r$	5/2
Kep4	Keplerian 5:2 forced	$\nu_L = \nu_r$	$\nu_U = \nu_k - \nu_r$	5/2
Ep5	epicyclic 5:3 forced	$\nu_L = \nu_\theta - \nu_r$	$\nu_U = \nu_r$	5/3
Kep5	Keplerian 5:3 forced	$\nu_L = \nu_k - \nu_r$	$\nu_U = \nu_r$	5/3

3. Keplerian models

In this section we examine the predictions of the forced resonance models assuming Keplerian and radial epicyclic oscillations. Paper I illustrates that the 3:2 parametric Kep model implies a much simpler behaviour of the $M \times \nu_U(a)$ relation than the 3:2 parametric Ep model. This is also true for the forced resonance models. As noted by Török & Stuchlík (2005), the ratio between Keplerian frequency and radial (or vertical) epicyclic frequency is a monotonic function of orbital radius r for any value of $a \in [0, \infty)$. For this reason, there is always a unique QPO excitation radius $\tilde{r}_{p:q}$ for any Kep model.

In the particular case of the 3:1 forced Keplerian resonance model (Kep1 model), the resonance occurs at the $\tilde{r}_{3:1}$ orbit where

$$\nu_k = 3\nu_r \tag{5}$$

and we can express the observed 3:2 QPO frequencies in the same manner as Kluźniak & Abramowicz (2001),

$$\nu_L = \nu_k - \nu_r, \text{ and } \nu_U = \nu_k. \tag{6}$$

Solving Eq. (5) yields the relation between spin and dimensionless resonant radius $\tilde{x}_{3:1} \equiv \tilde{r}_{3:1}/M$,

$$a = \frac{\sqrt{\tilde{x}_{3:1}}}{9}\left(12 \mp \sqrt{6(4\tilde{x}_{3:1} - 3)}\right), \tag{7}$$

where the "–" sign holds for $a \leq \tilde{a}_{3:1} = 1.1547$. The associated $\tilde{x}_{3:1}(a)$ function is shown in Fig. 2a. Figure 2b then shows the related $M \times \nu_U(a)$ function exhibiting its maximum for $1 \lesssim a \approx \tilde{a}_{3:1}$.

The other four Kep models (Kep2–Kep5) exhibit qualitatively similar behaviour of resonant radii to that of the Kep1 model. In full analogy, $M \times \nu_U(a)$ relations are then also represented by single continuous functions having a maximum close to $1 \lesssim a \approx \tilde{a}_{p:q}$. In Table 2 we specify relations between the spin and resonant radii calculated for each of the Kep1–Kep5 models. Illustrations of relevant $M \times \nu_U(a)$ relations are included in Fig. 2.

4. Epicyclic models

In analogy to Eq. (5), for the 3:1 forced epicyclic resonance model (Ep1 model), the resonance occurs at the $r_{3:1}$ orbit where we have

$$\nu_\theta = 3\nu_r \tag{8}$$

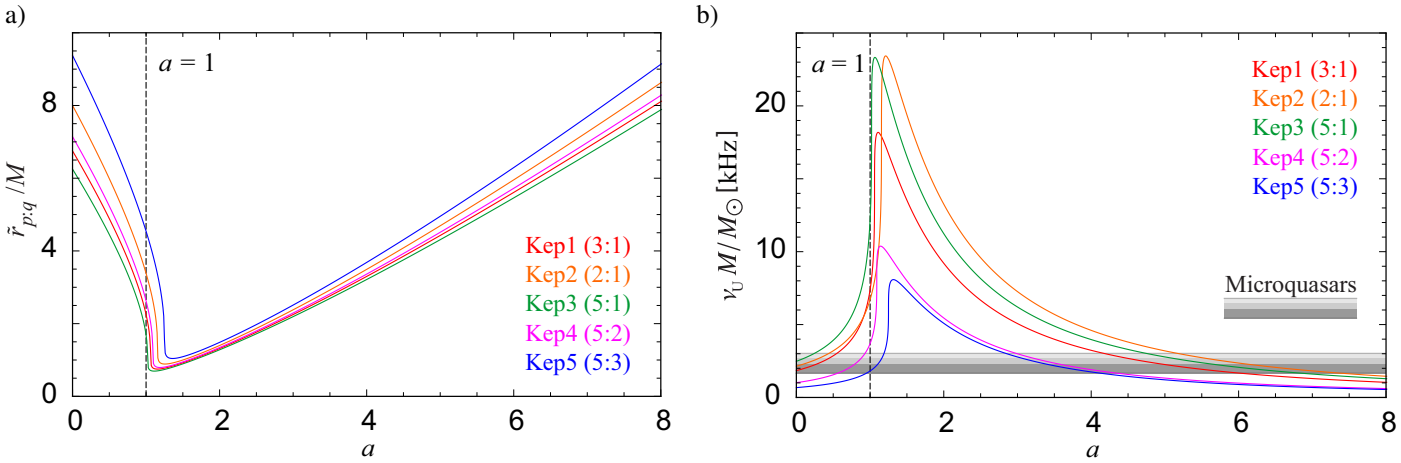

Fig. 2. *Panel a*: resonant radii of Kep models calculated in Kerr spacetimes. *Panel b*: resonant frequencies of Kep models calculated in Kerr spacetimes. The shaded region corresponds to observational values of $\nu_U \times M$ determined for Galactic microquasars (see Fig. 4 for details and Sect. 5 for a discussion).

Table 2. Spin functions $a(\tilde{x}_{p:q})$ determined for the Keplerian forced resonance QPO models.

Model	Spin function	$\tilde{a}_{p:q}$
Kep1	$a(\tilde{x}_{3:1}) = \frac{\sqrt{\tilde{x}_{3:1}}}{9}\left(12 \mp \sqrt{6(4\tilde{x}_{3:1} - 3)}\right)$	1.15470
Kep2	$a(\tilde{x}_{2:1}) = \frac{\sqrt{\tilde{x}_{2:1}}}{6}\left(8 \mp \sqrt{9\tilde{x}_{2:1} - 8}\right)$	1.25708
Kep3	$a(\tilde{x}_{5:1}) = \frac{\sqrt{\tilde{x}_{5:1}}}{15}\left(20 \mp \sqrt{2(36\tilde{x}_{5:1} - 25)}\right)$	1.11111
Kep4	$a(\tilde{x}_{5:2}) = \frac{\sqrt{\tilde{x}_{5:2}}}{15}\left(20 \mp \sqrt{63\tilde{x}_{5:2} - 50)}\right)$	1.18783
Kep5	$a(\tilde{x}_{5:3}) = \frac{\sqrt{\tilde{x}_{5:3}}}{15}\left(20 \mp \sqrt{2(24\tilde{x}_{5:3} - 25)}\right)$	1.36083

Notes. There are two separate branches of solution for each model, the "−" sign applies to black holes and naked singularities with $1 < a \lesssim \tilde{a}_{p:q}$, while the "+" sign applies to naked singularities with $a \gtrsim \tilde{a}_{p:q}$. The last column indicates the value of $\tilde{a}_{p:q}$ for each model.

and we can express the observed 3:2 QPO frequencies as Kluźniak & Abramowicz (2001),

$$\nu_L = \nu_\theta - \nu_r \text{ and } \nu_U = \nu_\theta. \tag{9}$$

Solving Eq. (8) yields the relation between the spin and dimensionless resonant radius $x_{3:1}$,

$$a = \frac{\sqrt{x_{3:1}}}{15}\left(19 \mp 2\sqrt{15x_{3:1} - 11}\right), \tag{10}$$

where the "−" sign holds for $a \leq a_{3:1} = 1.08471$.

The behaviour of relation (10) is shown in Fig. 3a together with relations obtained for the other four Ep models. On a large scale of a, the displayed curves are similar to those drawn for the Kep models in Fig. 2a. However, there is a qualitative difference which is emphasized within the enlarged area in Fig. 3a. For $a \gtrsim 1$, each of Ep models exhibits "S-like" behaviour of resonant radii. In contrast to Kep models, the resonance radius is not a single function of spin because of the non-monotonic behaviour of the ratio between epicyclic frequencies noted and discussed by Török & Stuchlík (2005) and Stuchlík et al. (2013). We find that for Ep models and $1 \lesssim a \lesssim a^*_{p:q}$ three distinct branches of $x_{p:q}(a)$ appear. This is illustrated in detail for the Ep1 model in Fig. 3b.

Table 3. Spin functions $a(x_{p:q})$ determined for the epicyclic forced resonance QPO models.

Model	Spin function	$a_{p:q}$ $a^*_{p:q}$
Ep1	$a(x_{3:1}) = \frac{\sqrt{x_{3:1}}}{15}\left(19 \mp 2\sqrt{15x_{3:1} - 11}\right)$	1.08471 1.00119
Ep2	$a(x_{2:1}) = \frac{\sqrt{x_{2:1}}}{5}\left(6 \mp \sqrt{5x_{2:1} - 4}\right)$	1.07331 1.01193
Ep3	$a(x_{5:1}) = \frac{\sqrt{x_{5:1}}}{13}\left(17 \mp 2\sqrt{13x_{5:1} - 9}\right)$	1.08807 1.00006
Ep4	$a(x_{5:2}) = \frac{\sqrt{x_{5:2}}}{29}\left(36 \mp \sqrt{7(29x_{5:2} - 22)}\right)$	1.08123 1.00337
Ep5	$a(x_{5:3}) = \frac{\sqrt{x_{5:3}}}{51}\left(59 \mp 2\sqrt{2(51x_{5:3} - 43)}\right)$	1.06226 1.03363

Notes. There are two separate branches of solution for each model, the "−" sign applies to black holes and naked singularities with $1 < a \lesssim a_{p:q}$, while the "+" sign applies to naked singularities with $a \gtrsim a_{p:q}$. The last column indicates the value of $a_{p:q}$ for each model as well as the related spin value $a^*_{p:q}$, where the $a(x_{p:q})$ function has a local maximum, which implies the "S-like" behaviour of resonant radii $x_{p:q}(a)$ and the existence of three resonant radii for $1 \lesssim a \lesssim a^*_{p:q}$ (see Fig. 3b).

We specify the relations between the spin and resonant radii calculated for each of the Ep1–Ep5 models in Table 3.

The behaviour of resonant frequencies $\nu_U(a)$ implied by Ep models displayed in Fig. 3 is more complex than that implied by Kep models. In analogy to the comparison between the behaviours of resonant radii, on a large scale of a, there is a similarity between the behaviours of frequencies predicted by both Kep and Ep models (see Figs. 2b and 4a). It can also be found that there is a clear qualitative difference for $a \sim 1$. Even for $a \lesssim 1$, only the Ep2 and Ep5 models imply qualitatively

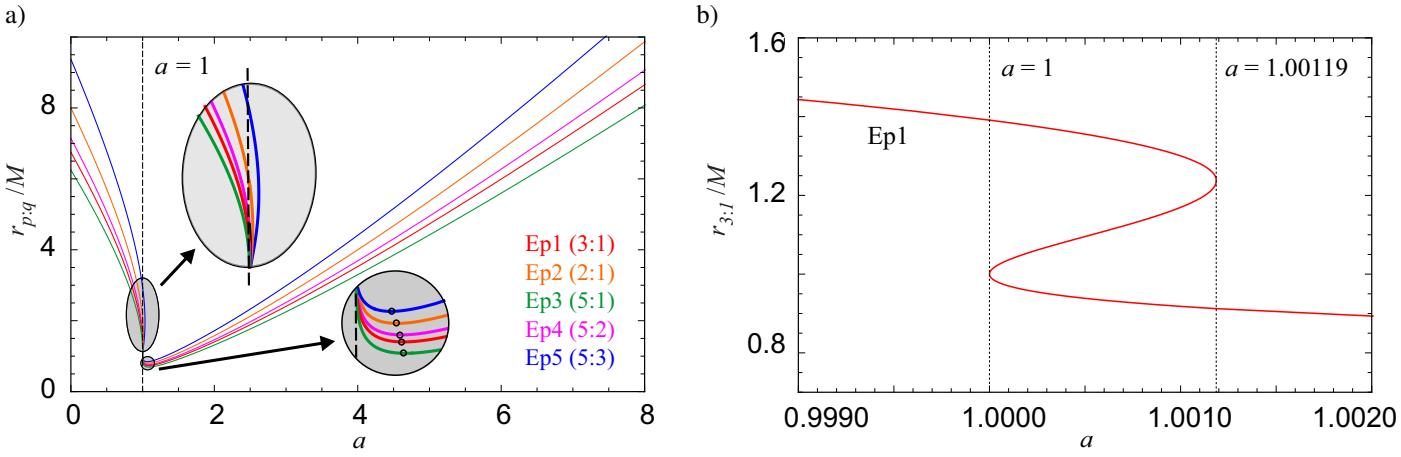

Fig. 3. *Panel a*: resonant radii of Ep models calculated in Kerr spacetimes. The enlarged area emphasizes a region close to $a = 1$ where each $a(r_{p:q})$ function exhibits both a local minimum and a local maximum. Global minima of $r_{p:q}(a)$ functions are denoted by circles. *Panel b*: detailed view of the behaviour of the $r_{3:1}(a)$ relation for $a \approx 1$. The global minimum of $r_{3:1}$ is not shown since it occurs only for a higher value of spin, $a_{3:1} = 1.08471$.

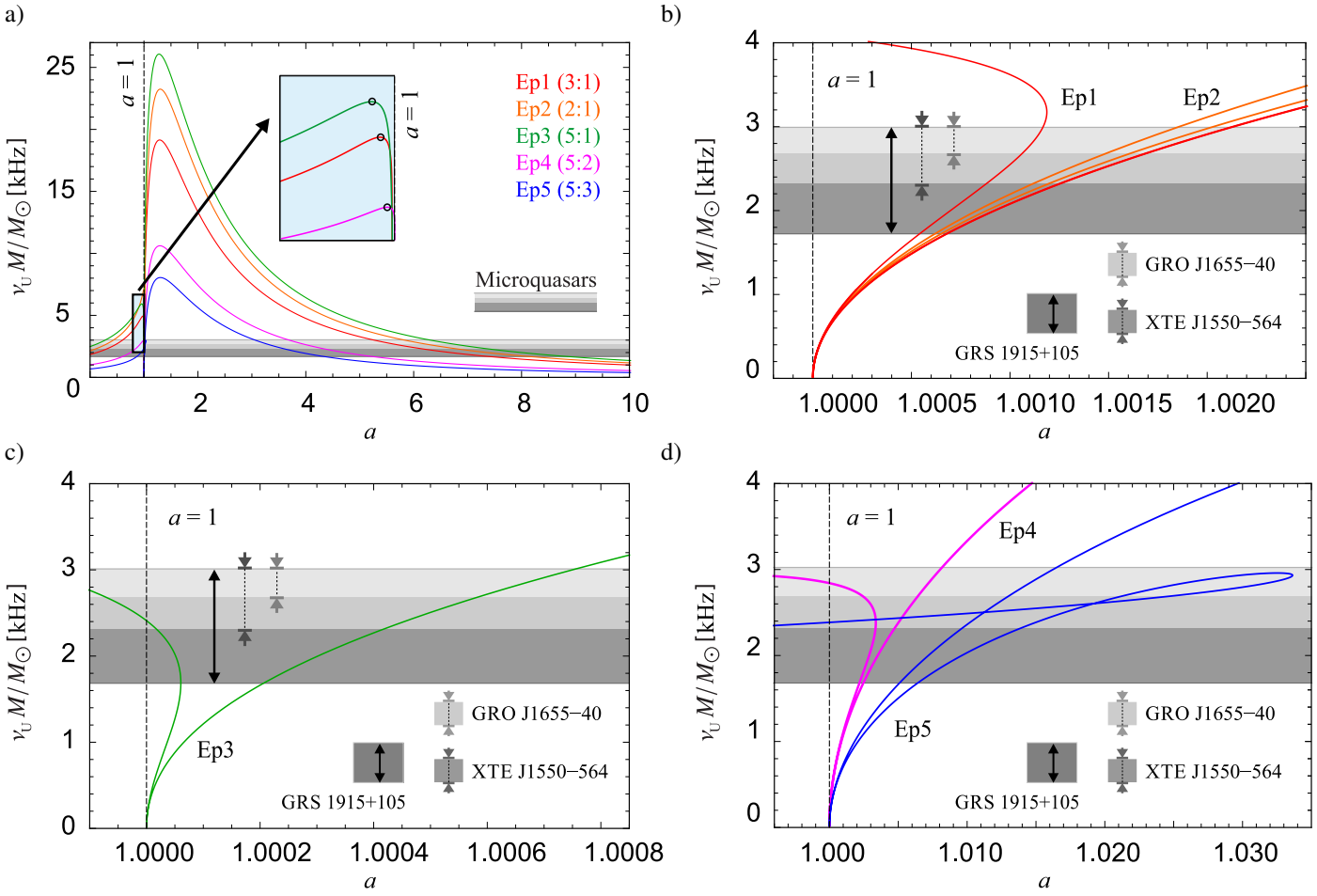

Fig. 4. Resonant frequencies of the Ep models calculated in Kerr spacetimes. The enlarged area emphasizes the existence of maxima of the $\nu_U \times M$ curves in the case of the Ep1, Ep3, and Ep4 models in BH spacetimes. The shaded region corresponds to the observational values of $\nu_U \times M$ determined for Galactic microquasars (see Sect. 5 for discussion). *Panel a*: behaviour of resonant frequencies of the whole group of models on a large scale of a. *Panel b*: detailed view of behaviour of the resonant frequencies for the Ep1 and Ep2 models for $a \approx 1$. The individual horizontal grey-scaled areas denote the observational values of $\nu_U \times M$ determined for each of the Galactic microquasars. *Panel c*: detailed view of the behaviour of resonant frequencies for the Ep3 model for $a \approx 1$. *Panel d*: detailed view of the behaviour of resonant frequencies for the Ep4 and Ep5 models for $a \approx 1$.

the same monotonic increase in ν_U with increasing a as in the Kep models. The other three Ep models (Ep1, Ep3, and Ep4) display sharp maxima of $\nu_U(a)$ for rapidly rotating Kerr BHs (see the enlarged area in Fig. 4a). The existence of these maxima is a consequence of the existence of the maximum of the vertical epicyclic frequency $\nu_\theta(r)$ discussed by Török & Stuchlík (2005).

Table 4. Spin intervals inferred for the three microquasars (GRS 1915+105, XTE J1550−564, and GRO J1655−40) from the individual Ep and Kep models.

Model	GRS 1915+105		XTE J1550−564		GRO J1655−40	
Ep1	<0.61		0.32−0.59		0.50−0.59	
	1.00052−1.00217	5.25−7.40	1.00088−1.00116		1.00107−1.00116	
			1.00125−1.00210	5.29−6.13	1.00171−1.00209	5.30−5.61
Ep2	<0.44		0.11−0.42		0.31−0.42	
	1.00059−1.00207	5.81−8.14	1.00111−1.00200	5.86−6.77	1.00151−1.00199	5.87−6.20
Ep3	<0.29		<0.27		0.13−0.26	
	0.99978−1.00006		0.99980−1.00002		0.99981−0.99992	
	1.00020−1.00076	6.28−8.85	1.00042−1.00074	6.34−7.34	1.00059−1.00073	6.35−6.72
Ep4	0.60490−1.00818	3.68−5.23	0.84716−1.00337		0.93259−1.00233	
			1.00474−1.00794	3.71−4.32	1.00647−1.00788	3.72−3.94
Ep5	0.86756−1.03363	3.05−4.34	0.99257−1.03363	3.08−3.59	1.01310−1.01590	
					1.02148−1.03363	3.08−3.27
Kep1	<0.55	4.17−5.99	0.29−0.54	4.21−4.92	0.45−0.53	4.22−4.48
Kep2	<0.44	5.17−7.34	0.12−0.43	5.22−6.06	0.31−0.42	5.23−5.54
Kep3	<0.24	4.75−6.81	<0.23	4.79−5.59	0.11−0.22	4.80−5.09
Kep4	0.57−0.93	2.98−4.33	0.80−0.93	3.01−3.54	0.88−0.92	3.02−3.21
Kep5	0.95615−1.18902	2.84−4.10	1.11049−1.18574	2.87−3.36	1.16028−1.18489	2.87−3.05

For $1 \lesssim a \lesssim a^{*}_{p:q}$, the $M \times \nu_{U}(a)$ curves then have the same topology for the Ep1, Ep3, and Ep4 models, and two additional and different topologies for the Ep2 and Ep5 models. These topologies are illustrated in Figs. 4b–d.

5. Discussion and conclusions

As discussed in detail in Paper I, numerous attempts to estimate the spin a of black hole candidates have been undertaken using the iron-line profile, the X-ray continuum, or the QPO frequency fitting-methods. In Paper I we attempted to extend the application of the X-ray timing approach to super-spinning compact objects with exteriors described by the spacetime of a Kerr naked singularity and interior given by the solutions of string theory. We discussed there various types of QPO models including several resonance models and concluded that the Ep and Kep models are favoured in the context of the $a > 1$ hypothesis. Here we extended our consideration and investigated in a consistent way the implications of a set of ten forced resonance models including five Kep and five Ep models so far discussed only in the context of $a < 1$. We applied the same physical arguments to these models as used in Paper I. In particular, we assumed that only a small deviation of spin estimate from $a = 1$, $a \gtrsim 1$ could occur for a favoured model, as is often considered in the case of super-spinning relativistic compact objects (Calvani & Nobili 1979; Stuchlík 1980, 1981; Stuchlík et al. 2011; see discussion in Paper I).

Predictions of these ten newly considered models are illustrated in Figs. 2–4. The observationally determined ranges of $M \times \nu_{U}(a)$ for each of the Galactic microquasars are denoted in Figs. 2b and 4 by the individual horizontal grey-scaled areas. For a particular QPO model and source with an independently estimated mass range we calculated the relevant spin interval of the central compact object as predicted by the concrete model. The results are summarized in Table 4 and show that there could be two (for the Kep models) or up to four (for the Ep models) different spin intervals for each QPO model. The number of the relevant spin intervals and their ranges depend on the topology of the $M \times \nu_{U}(a)$ relation and on the observed range of mass for a given source. Confronting the QPO models predictions with the data of Galactic microquasars[2], we find that each of these models is compatible with the assumption of $a > 1$, but only some of them with the assumption of $a \gtrsim 1$.

Comparing our new results with the results obtained in Paper I, we conclude that five Keplerian forced resonance models (Kep1–Kep5) show qualitatively similar behaviour with the 3:2 parametric Keplerian model (Kep) considered in Paper I. More specifically, for all the Kep models we find the existence of a unique QPO excitation radius $\tilde{r}_{p:q}$ and consequent simple behaviour of $M \times \nu_{U}(a)$ relations represented by a single function having solely one maximum close to $a \gtrsim 1$. Inspecting the resonant frequencies drawn in Fig. 2b and the results given in Table 4 we can find that only one of the Keplerian forced resonance models (Kep5) is compatible with the expectation of $a \gtrsim 1$ and gives quantitatively similar results to the 3:2 parametric Keplerian model (Kep) considered in Paper I. For the other four Kep models (Kep1–Kep4), the inferred values of spin are either lower or several times higher than the extreme Kerr black hole value $a = 1$. Therefore, for the case of the three Galactic microquasars considered here, these four Kep models can be ruled out from further consideration.

[2] The assumed values of the measured mass and QPO frequencies of each microquasar are summarized in Table 1 of Paper I, and follow from the studies of Greene et al. (2001), Greiner et al. (2001), Strohmayer (2001), Orosz et al. (2002), Remillard et al. (2002), McClintock & Remillard (2006).

On the other hand, from our results given in Fig. 4 and Table 4, we can see that each of the five epicyclic forced resonance models (Ep1–Ep5) is compatible with the expectation of $a \gtrsim 1$, and thus none of them can be ruled out. The Ep models imply the existence of multiple resonant radii and therefore more complicated $M \times \nu_{\rm U}(a)$ relations than those implied by the Kep models. The Ep1–Ep5 models are similar to the 3:2 parametric epicyclic model (Ep) considered in Paper I. However, as elaborated in Sect. 4, the Ep models in general allow a very wide variety of topologies of the $M \times \nu_{\rm U}(a)$ relation. The relation explored in Paper I for the Ep model corresponds to only one specific topology from this variety. For the Ep models considered here, three different topologies are possible and for only one of them (Ep5) the $M \times \nu_{\rm U}(a)$ relation has the same topology as that explored in Paper I.

For all the Ep models, there is the possibility of recognizing a direct observational signature of presence of a super-spinning compact object. It is clear from Figs. 4b–d that more pairs of different 3:2 commensurable frequencies can be expected within a single source. In a full analogy to the specific case of Ep model discussed in Paper I, we conclude that this issue can be resolved using the large amount of high-quality data available from the next generation of X-ray observatories including technologies such as the proposed concept of Large Area Detector (Feroci et al. 2012, 2014; Zhang et al. 2016).

Spin intervals implied by 3:2 or 2:3 QPOs. The results presented in Table 4 assume that the predicted pair of QPO frequencies forms the 3:2 ratio, whereas the frequency denoted in Table 1 as $\nu_{\rm U}$ is higher than that denoted as $\nu_{\rm L}$. However, some of the considered models imply that there can be an inverse inequality, $\nu_{\rm L}/\nu_{\rm U} = 3/2$. We have investigated this possibility and found that four models are compatible with observation. Specifically, for the Kep4 model the implied spin intervals are then the same as those given in Table 4 for the Kep5 model and vice versa. A fully analogous conclusion also holds for the Ep4 and Ep5 models.

Acknowledgements. We would like to acknowledge the Czech grant GAČR 17-16287S, "Oscillations and coherent features in black-hole accretion disks and their observational signatures". We thank to the INTER-EXCELLENCE project No. LTI17018 which supports international activities of the Silesian University in Opava (SU) and Astronomical Institute in Prague (ASU). We also acknowledge two internal SU grants, SGS/14,15/2016 and IGS/2/2016. Z.S. acknowledges the Albert Einstein Center for Gravitation and Astrophysics supported by the Czech Science Foundation grant No. 14-37086G. We are grateful to Marek Abramowicz (Nicolaus Copernicus Astronomical Center in Warsaw – CAMK & SU), Wlodek Kluźniak (CAMK), Maciek Wielgus (CAMK), Jiří Horák (ASU), and Pavel Bakala (SU) for many useful discussions. Furthermore we would like to acknowledge the hospitality of CAMK. We express our sincere thanks to the concierges of the Mlýnská hotel in Uherské Hradiště, Czech Republic for their kind help and participation in organizing frequent workshops of SU and ASU. Last but not least, the authors wish to thank the anonymous referee for the useful and constructive comments that substantially helped to improve the manuscript.

References

Abramowicz, M. A., & Kluźniak, W. 2001, A&A, 374, L19
Abramowicz, M. A., Almergren, G. J. E., Kluźniak, W., Thampan, A. V., & Wallinder, F. 2002, CQG, 19, L57
Abramowicz, M. A., Bulik, T., Bursa, M., & Kluźniak, W. 2003a, A&A, 404, L21
Abramowicz, M. A., Karas, V., Kluźniak, W., Lee, W. H., & Rebusco, P. 2003b, PASJ, 55, 467
Abramowicz, M. A., Kluźniak, W., McClintock, J. E., & Remillard, R. A. 2004, ApJ, 609, L63
Aliev, A. N., & Galtsov, D. V. 1981, GRG, 13, 899
Aschenbach, B., Grosso, N., Porquet, D., & Predehl, P. 2004, A&A, 417, 71
Bambi, C. 2011, Europhys. Lett., 94, 50002
Bambi, C. 2012, J. Cosmol. Astropart. Phys., 9, 14
Bambi, C. 2014, Phys. Lett. B, 730, 59
Bambi, C., & Freese, K. 2009, PRD, 79, 043002
Calvani, M., & Nobili, L. 1979, Nuovo Cimento B Serie, 51, 247
Done, C., Gierliński, M., & Kubota, A. 2007, A&ARv, 15, 1
Feroci, M., Stella, L., van der Klis, M., et al. 2012, Exp. Astron., 34, 415
Feroci, M., den Herder, J. W., Bozzo, E., et al. 2014, in Space Telescopes and Instrumentation 2014: Ultraviolet to Gamma Ray, Proc. SPIE, 9144, 91442T
Gilfanov, M., Churazov, E., & Revnivtsev, M. 2000, MNRAS, 316, 923
Gimon, E. G., & Hořava, P. 2009, Phys. Lett. B, 672, 299
Greene, J., Bailyn, C. D., & Orosz, J. A. 2001, ApJ, 554, 1290
Greiner, J., Cuby, J. G., & McCaughrean, M. J. 2001, Nature, 414, 522
Horák, J. 2004, in RAGtime 4/5: Workshops on Black Holes and Neutron Stars, eds. S. Hledík, & Z. Stuchlík, 91
Horák, J. 2005, Astron. Nachr., 326, 824
Horák, J. 2008, A&A, 486, 1
Horák, J., & Karas, V. 2006, A&A, 451, 377
Horák, J., & Lai, D. 2013, MNRAS, 434, 2761
Horák, J., Abramowicz, M. A., Kluźniak, W., Rebusco, P., & Török, G. 2009, A&A, 499, 535
Ingram, A., & Done, C. 2010, MNRAS, 405, 2447
Ingram, A., & Done, C. 2011, MNRAS, 415, 2323
Ingram, A., Done, C., & Fragile, P. C. 2009, MNRAS, 397, L101
Ingram, A., van der Klis, M., Middleton, M., et al. 2016, MNRAS, 461, 1967
Johannsen, T. 2016, CQG, 33, 124001
Johannsen, T., & Psaltis, D. 2011, ApJ, 726, 11
Kato, S. 2004, PASJ, 56, L25
Kluźniak, W., & Abramowicz, M. A. 2001, ArXiv e-prints [arXiv:astro-ph/0105057]
Kluźniak, W., & Abramowicz, M. A. 2002, ArXiv e-prints [arXiv:astro-ph/0203314]
Kluźniak, W., & Abramowicz, M. A. 2005, Ap&SS, 300, 143
Kološ, M., & Stuchlík, Z. 2013, PRD, 88, 065004
Kotrlová, A., Stuchlík, Z., & Török, G. 2008, CQG, 25, 225016
Kotrlová, A., Török, G., Šrámková, E., & Stuchlík, Z. 2014, A&A, 572, A79
Li, Z., & Bambi, C. 2013a, PRD, 87, 124022
Li, Z., & Bambi, C. 2013b, J. Cosmol. Astropart. Phys., 3, 31
McClintock, J. E., & Remillard, R. A. 2006, in Compact Stellar X-ray Sources, eds. W. Lewin, & M. van der Klis (Cambridge, UK: Cambridge University Press), Cambridge Astrophys. Ser., 39, 157
McClintock, J. E., Narayan, R., & Shafee, R. 2007, ArXiv e-prints [arXiv:0707.4492]
McClintock, J. E., Narayan, R., Gou, L., et al. 2010, X-ray Astronomy 2009, Present Status, Multi-Wavelength Approach and Future Perspectives, 1248, 101
McClintock, J. E., Narayan, R., Davis, S. W., et al. 2011, CQG, 28, 114009
McClintock, J. E., Narayan, R., & Steiner, J. F. 2014, Space Sci. Rev., 183, 295
Middleton, H., Del Pozzo, W., Farr, W. M., Sesana, A., & Vecchio, A. 2006, MNRAS, 455, L72
Miller, J. M. 2007, ARA&A, 45, 441
Montero, P. J., Zanotti, O., Font, J. A., & Rezzolla, L. 2007, MNRAS, 378, 1101
Motta, S. E., Muñoz-Darias, T., Sanna, A., et al. 2014, MNRAS, 439, L65
Nowak, M., & Lehr, D. 1999, in Theory of Black Hole Accretion Disks, eds. M. A. Abramowicz, G. Björnsson, & J. E. Pringle (Cambridge: Cambridge University Press), 21
Orosz, J. A., Groot, P. J., van der Klis, M., et al. 2002, ApJ, 568, 845
Ortega-Rodríguez, M., Solís-Sánchez, H., López-Barquero, V., Matamoros-Alvarado, B., & Venegas-Li, A. 2014, MNRAS, 440, 3011
Psaltis, D., Perrodin, D., Dienes, K. R., & Mocioiu, I. 2008, PRL, 100, 091101
Rebusco, P. 2004, PASJ, 56, 553
Rebusco, P. 2008, New Astron. Rev., 51, 855
Remillard, R. A., Muno, M. P., McClintock, J. E., & Orosz, J. A. 2002, ApJ, 580, 1030
Rezzolla, L., Yoshida, S., & Zanotti, O. 2003, MNRAS, 344, 978
Schnittman, J. D., & Rezzolla, L. 2006, ApJ, 637, L113
Shafee, R., McKinney, J. C., Narayan, R., et al. 2008, ApJ, 687, L25
Šrámková, E. 2005, Astron. Nachr., 326, 835
Šrámková, E., Torkelsson, U., & Abramowicz, M. A. 2007, A&A, 467, 641
Steiner, J. F., Reis, R. C., McClintock, J. E., et al. 2011, MNRAS, 416, 941
Strohmayer, T. E. 2001, ApJ, 552, L49
Stuchlík, Z. 1980, Bull. Astron. Inst. Czechoslovakia, 31, 129
Stuchlík, Z. 1981, Bull. Astron. Inst. Czechoslovakia, 32, 68
Stuchlík, Z., & Kološ, M. 2016a, APJ, 825, 13
Stuchlík, Z., & Kološ, M. 2016b, A&A, 586, A130
Stuchlík, Z., & Kotrlová, A. 2009, GRG, 41, 1305
Stuchlík, Z., & Schee, J. 2010, Class. Quant. Grav., 27, 215017
Stuchlík, Z., & Schee, J. 2012a, Class. Quant. Grav., 29, 025008

Stuchlík, Z., & Schee, J. 2012b, Class. Quant. Grav., 29, 065002
Stuchlík, Z., & Schee, J. 2013, Class. Quant. Grav., 30, 075012
Stuchlík, Z., Kotrlová, A., & G. Török. 2008, Acta Astron., 58, 441
Stuchlík, Z., Hledík, S., & Truparová, K. 2011, Class. Quant. Grav., 28, 155017
Stuchlík, Z., Kotrlová, A., & Török, G. 2013, A&A, 552, A10
Stuchlík, Z., Kotrlová, A., Török, G., & Goluchová, K. 2014, Acta Astron., 64, 45
Török, G. 2005a, A&A, 440, 1
Török, G. 2005b, Astron. Nachr., 326, 856
Török, G., & Stuchlík, Z. 2005, A&A, 437, 775
Török, G., Abramowicz, M. A., Kluźniak, W., & Stuchlík, Z. 2005, A&A, 436, 1
Török, G., Kotrlová, A., Šrámková, E., & Stuchlík, Z. 2011, A&A, 531, A59
Török, G., Goluchová, K., Horák, J., et al. 2016, MNRAS, 457, L19
van der Klis, M. 2006, in Compact Stellar X-ray Sources, eds. W. Lewin, & M. van der Klis (Cambridge, UK: Cambridge University Press), Cambridge Astrophys. Ser., 39
Vio, R., Rebusco, P., Andreani, P., Madsen, H., & Overgaard, R. V. 2006, A&A, 452, 383
Wagoner, R. V. 2012, ApJ, 752, L18
Wagoner, R. V., Silbergleit, A. S., & Ortega-Rodríguez, M. 2001, ApJ, 559, L25
Yagi, K., & Stein, L. C. 2016, Class. Quant. Grav., 33, 054001
Zanotti, O., Font, J. A., Rezzolla, L., & Montero, P. J. 2005, MNRAS, 356, 1371
Zhang, S. N., Feroci, M., Santangelo, A., et al. 2016, in Society of Photo-Optical Instrumentation Engineers (SPIE) Conf. Ser., Proc. SPIE, 9905, 99051Q
Zhou, X.-L., Yuan, W., Pan, H.-W., & Liu, Z. 2015, ApJ, 798, L5